Determination of the Relative Orientation of the Two Halves of the Domain-Swapped Dimer of Cyanovirin-N in Solution Using Dipolar Couplings and Rigid Body Minimization

Carole A. Bewley*,† and **G. Marius Clore*,‡**

Contribution from the Laboratories of Bioorganic Chemistry and Chemical Physics, National Institute of Diabetes and Digestive and Kidney Diseases, National Institutes of Health, Bethesda, Maryland 20892

Abstract: The HIV-inactivating protein cyanovirin-N (CVN) exists in two forms that are pH- and solvent-dependent: a monomer which predominates at neutral pH (≥90%) and a symmetric domain-swapped dimer. We have investigated the orientation of the two halves of the domain-swapped dimer of CVN at neutral pH in solution using dipolar couplings measured in a neutral liquid crystalline bicelle medium. $^1D_{NH}$ dipolar couplings for the dimer were readily measured for 18 out of 101 residues, and are shown to be inconsistent with the orientation of the two halves of the dimer observed in the X-ray structure obtained from crystals grown at low pH in the presence of organic solvent. The orientation of the two halves of the domain-swapped dimer was determined by rigid body minimization, subject to the requirements of C_2 symmetry. The starting coordinates for the calculations consisted of the X-ray coordinates for the two halves (with the linker residues deleted), separated by ∼45 Å and placed in three different relative orientations. One-half of the dimer is held fixed, the other half is free to rotate and translate (6 degrees of freedom), and the alignment tensor for the dipolar couplings is free to rotate (3 degrees of freedom). The target function comprised only four terms: dipolar coupling restraints (18 × 2), distance restraints (12) to link the two halves and to prevent steric clash, a radius of gyration restraint to achieve appropriate compaction, and a quartic van der Waals repulsion term. Structures were calculated for different target values of the radius of gyration, and back-calculation of the alignment tensor and dipolar couplings on the basis of molecular shape was used to filter the resulting structures. Prediction of dipolar couplings in this manner is predicated on the assumption that orientational order is dictated by steric interactions between the liquid crystalline medium and the protein. The validity of this assumption in this particular case is evidenced by the excellent agreement between predicted and observed dipolar couplings for the monomer. We show that the data is only consistent with a very small range of orientations of the two halves of the dimer in which the angle between the long axes of the two halves is ∼110°. The relative orientation of the two halves of the dimer at neutral pH in solution is quite different from that observed in the crystals obtained at low pH in organic solvent. The factors stabilizing the relative orientation of the two halves of the dimer under different conditions are discussed. The methodology presented in this paper should find a wide range of applicability to numerous other structural problems involving multimeric proteins and protein−protein complexes.

Introduction

Cyanovirin-N (CVN) is a potent HIV-inactivating protein isolated from the cyanobacterium *Nostoc ellipsosporum*,[1] which has been shown to exist in two forms: an 11 kDa monomer[2] and a 22 kDa domain-swapped dimer.[3] At neutral pH, the monomeric form is predominant (≥90%).[3] The domain-swapped

dimeric form can be formed at low pH (<3.5) under certain specific conditions involving the presence of some organic solvent such as those pertaining to reverse-phase HPLC (acetonitrile−water gradient) or crystallization (26% 2-propanol).[3] The structure of the monomeric form was solved by NMR[2] (Figure 1a) and that of the dimeric form by X-ray crystallography[3] (Figure 1b). The structure of the monomer in solution is essentially identical to that of the AB′ (or A′B) half of the dimer (Figure 1),[2] where A and A′ comprise residues 1−50 of each subunit, and B and B′ residues 52−101 of each subunit. Thus, in the domain-swapped dimer, residues 1−50 of one subunit and 52′−101′ of the other subunit correspond to the structure of the monomer. The two halves of the dimer (AB′ and A′B) in the crystal are oriented at ∼80° relative to each other (Figure 1b). This orientation is stabilized by a hydrogen bond between the neutral carboxylic acid moiety of Glu41 of one subunit and Glu41′ of the other as well as by the presence of a tightly packed neighbor in the crystal lattice (Figure 1b). At neutral pH, however, the orientation of the two halves of

* To whom correspondence should be addressed. (C.A.B.) Telephone: (301) 594-5187. Fax: (301) 402-0008. E-mail: bewley@speck.niddk.nih.gov. (G.M.C.) Telephone (301) 496-0782. Fax: (301) 496-0825. E-mail: clore@speck.niddk.nih.gov.
† Laboratory of Bioorganic Chemistry.
‡ Laboratory of Chemical Physics.

(1) Boyd, M. R.; Gustafson, K. R.; McMahon, J. B.; Shoemaker, R. H.; O'Keefe, B. R.; Mori, T.; Gulakowski, R. J.; Wu, L.; Rivera, M. I.; Laurencot, C. M.; Currens, M. J.; Cardellina, J. H.; Buckheit, R. W.; Nara, P. L.; Pannell, L. K.; Sowder, R. C.; Henderson, L. E. *Antimicrob. Agents Chemother.* **1997,** *41,* 1521−1530.
(2) Bewley, C. A.; Gustafson, K. R.; Boyd, M. R.; Covell, D. G.; Bax, A.; Clore, G. M.; Gronenborn, A. M. *Nat. Struct. Biol.* **1998,** *5,* 571−578.
(3) Yang, F.; Bewley, C. A.; Louis, J. M.; Gustafson, K. R.; Boyd, M. R.; Gronenborn, A. M.; Clore, G. M.; Wlodawer, A. *J. Mol. Biol.* **1999,** *288,* 403−412.
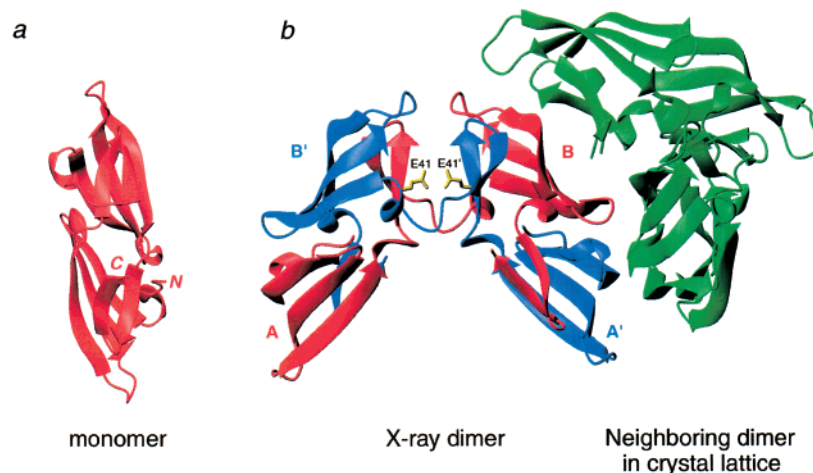
Figure 1. Ribbon diagrams illustrating the structures of (a) the monomeric and (b) the domain-swapped dimeric forms of CVN. The two subunits of the dimer are color coded in red (AB) and blue (A′B′). A and B comprise residues 1−50 and residues 52−101, respectively, linked by a Pro at position 51 (and likewise for A′ and B′). The monomer has the same structure as the AB′ (or A′B) half of the dimer, that is, residues 1−50 of one subunit and 52′−101′ of the other form a unit that has the same structure as the monomer. Also shown in (b) are the side chains of Glu41 and Glu41′ (in yellow) which are hydrogen-bonded at low pH, and the location of the neighboring dimer in the crystal lattice (green). Note that the open conformation of the X-ray dimer is stabilized by the insertion of half of one dimer (in this case the A′B half) between the two halves of the neighboring dimer (in green). The coordinates for the solution monomer are taken from ref 2 and for the X-ray dimer from ref 3.

the domain-swapped dimer observed in the crystal structure is likely to be destabilized in solution, owing to electrostatic repulsion between the two negatively charged carboxylates of Glu41 and Glu41′.

It has now been amply demonstrated that dipolar couplings provide unique long-range orientational restraints.[2,4−12] Moreover, it has recently been shown that accurate docking of protein−protein complexes can be achieved by rigid body minimization on the basis of orientational and translational restraints afforded by dipolar couplings and intermolecular NOEs.[13] In the case of the domain-swapped dimer of CVN we were unable to observe any NOEs between the AB′ and A′B halves since ≤10% of CVN is present in the dimeric form at neutral pH, and the interface between the AB′ and A′B halves is small. Hence, alternative translational restraints had to be employed, specifically in the form of distance restraints imposed by the covalent geometry of the domain-swapped dimer and a radius of gyration restraint to achieve appropriate packing.[14] In this paper, we make use of dipolar couplings and translational restraints, in conjunction with rigid body minimization and back-calculation of dipolar couplings based on molecular shape,[15] to determine the relative orientations of the two halves of the domain-swapped dimer of CVN in solution at neutral pH. We demonstrate unambiguously that the orientation of the two

halves of the domain-swapped dimer of CVN at neutral pH is quite different from that found in the crystal structure at low pH.
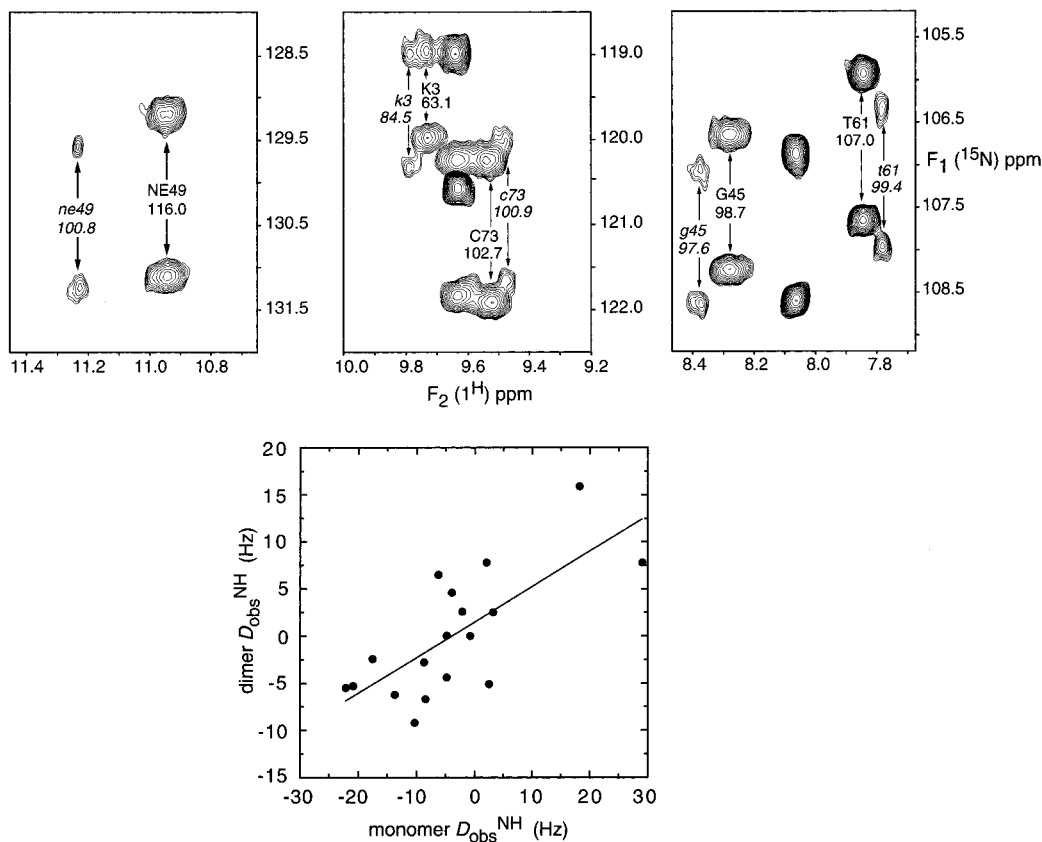
Results and Discussion

At neutral pH, approximately 10% of CVN exists as a domain-swapped dimer, the remainder being in the monomeric form.[3] The two forms are not interconvertible at neutral pH.[3] There are 18 peaks[16] in the ^{1}H−^{15}N correlation spectrum which are clearly doubled with peak ratios corresponding to the proportion of monomer and dimer determined by size exclusion chromatography (Figure 2). ^{15}N relaxation measurements (T_1 and $T_{1\rho}$) at 35 °C reveals that the major peaks correspond to the monomer with a rotational correlation time of ~4.5 ns, while the minor peaks correspond to the dimer with a rotational correlation time of ~10 ns.[17] The dipolar couplings measured for these 18 residues in a neutral liquid crystalline bicelle medium of 4.5% 3:1 DMPC:DHPC[4] are clearly different for the monomeric and dimeric forms and are only poorly correlated (Figure 2). A best-fit of the alignment tensor to the X-ray coordinates of the AB′ half of the dimer (which is equivalent to the monomer) using singular value decomposition (SVD)[18] yields a value of 14.2 Hz for the magnitude of the axial component of the alignment tensor (D_a^{NH}) and 0.29 for the rhombicity η (defined as the ratio of the rhombic to axial components of the traceless second rank tensor $\mathbf{D}_{NH}$) for the monomer dipolar couplings (Figure 3a).[19] For the dimer dipolar couplings the corresponding values are 7.6 Hz and 0.2, (Figure 3b).

(4) Tjandra, N.; Bax, A. *Science* **1997**, *278*, 1111−1114.

(5) Tjandra, N.; Omichinski, J. G.; Gronenborn, A. M.; Clore, G. M.; Bax, A. *Nat. Struct. Biol.* **1997**, *4*, 732−738.

(6) Clore, G. M.; Gronenborn, A. M. *Nat. Struct. Biol.* **1997**, *4 (Suppl. S)*, 849−853.

(7) Garrett, D. S.; Seok, Y.-J.; Peterkovsky, A.; Gronenborn, A. M.; Clore, G. M. *Nat. Struct. Biol.* **1998**, *6*, 166−173.

(8) Prestegard, J. H. *Nat. Struct. Biol.* **1998**, *5 (Suppl. S)*, 517−522.

(9) Clore, G. M.; Starich, M. R.; Bewley, C. A.; Cai, M.; Kuszewski, J. *J. Am. Chem. Soc.* **1999**, *21*, 6513−6514.

(10) Fischer, M. W. F.; Losonczi, J. A.; Weaver, J. L.; Prestegard, J. H. *Biochemistry* **1999**, *38*, 9013−9022.

(11) Al-Hashimi, H. M.; Bolon, P. J.; Prestegard, J. H. *J. Magn. Reson.* **2000**, *142*, 153−158.

(12) Skrynnikov, N. R.; Goto, N. K.; Yang, D.; Choi, W.-Y.; Tolman, J. R.; Mueller, G. A.; Kay, L. E. *J. Mol. Biol.* **2000**, *295*, 1265−1273.

(13) Clore, G. M. *Proc. Natl. Acad. Sci. U.S.A.* **2000**, in press.

(14) Kuszewski, J.; Gronenborn, A. M.; Clore, G. M. *J. Am. Chem. Soc.* **1999**, *121*, 2337−2338.

(15) Zweckstetter, M.; Bax, A. *J. Am. Chem. Soc.* **2000**, *122*, 3791−3792.

(16) The 18 residues in the dimer for which $^1D_{NH}$ dipolar couplings could be readily measured are as follows: the backbone amides of Lys3, Gly15, Ser33, Val43, Gly45, Leu47, Thr57, Thr61, Gln62, Ser67, Glu68, Cys73, Lys74, Asp88, Ile94, Thr97, and Glu101 and the side chain Nε1−Hε1 of Trp49.

(17) ^{15}N T_1 and $T_{1\rho}$ were measured as described by Tjandra, N.; Wingfield, P.; Stahl, S. J.; Bax, A. *J. Biomol. NMR* **1996**, *8*, 273−284. The rotational correlation time, τ_c, was determined by nonlinear least-squares best-fitting to either the $T_1/T_{1\rho}$ ratios and optimizing the value of τ_c, or to the individual T_1 and $T_{1\rho}$ values and optimizing the values of τ_c and the generalized order parameter S^2. The same values of τ_c were obtained by both methods.

(18) Losonczi, J. A.; Andrec, M.; Fischer, M. W. F.; Prestegard, J. H. *J. Magn. Reson.* **1999**, *138*, 334−342.

Figure 2. Three regions of the coupled $^1H-^{15}N$ correlation spectrum of CVN recorded in a bicelle liquid crystalline medium are shown in the top panels, illustrating the different dipolar couplings observed for the minor (~10%) dimeric form (annoted in small case italics) and the major (~90%) monomeric form (annotated in upper case letters). A plot of the 18 measured dipolar couplings for the dimer versus their equivalent measured values for the monomer is displayed in the bottom panel.

It has recently been shown that the alignment tensor and hence the dipolar couplings can be accurately predicted on the basis of molecular shape using a steric obstruction model, providing that there is no significant attractive or long-range repulsive interaction between the protein and the bicelle.[15] Back-calculation of the alignment tensor from the molecular shape of the monomer (i.e., using the X-ray coordinates of the AB′ half of the dimer) predicts a value of D_a^{NH} and η of 17.5 Hz and 0.1, respectively, with calculated dipolar couplings that agree well with the measured couplings for the monomer (Figure 3a) but poorly with those measured for the dimer (Figure 3b). This result indicates that orientational order of the CVN monomer is indeed dictated by steric interactions between the liquid crystalline medium and the protein. Since the chemical composition of the dimer is identical to that of the monomer and since the accessible surface of the dimer will have the same properties as the corresponding surfaces on the monomer, one can therefore safely assume that orientational order of the CVN dimer will also be dictated by steric interactions. Consequently, in this particular system back-calculation of dipolar couplings on the basis of molecular shape can safely be used as a filter for ascertaining the relative orientation of the two halves of the CVN dimer.

For a dimer with C_2 symmetry, one of the principal axes of the alignment tensor must be parallel and the other two orthogonal to the molecular 2-fold symmetry axis. If this were not the case, a 180° rotation about the 2-fold axis would change the orientation of the alignment tensor with respect to the dimer which is not possible since a 180° rotation leaves the body invariant (i.e., it is equivalent to a 360° rotation because of symmetry). In other words, for a single alignment tensor the dipolar couplings calculated for each half of the dimer must be identical. Even though only 18 dipolar couplings could be measured for the dimer, this requirement imposes a very severe restraint on the relative orientations of the two halves of the dimer. Since the observed monomer and dimer dipolar couplings are not consistent with those calculated from the X-ray dimer coordinates (i.e., the AB′ and A′B halves combined) using either best-fitting by SVD or back-calculation on the basis of molecular shape (Figure 3c and d), it follows that the relative orientation of the two halves of the dimer at neutral pH in solution must be different from that observed in the crystal. Moreover, the predicted value of D_a^{NH} back-calculated from the shape of the X-ray dimer is negative (−9 Hz) indicative of an oblate ellipsoid, whereas the actual value of D_a^{NH} (derived from an SVD fit to the monomer) is positive indicative of a prolate ellipsoid.

To determine the orientation of the two halves of the domain-swapped dimer in solution we used rigid body minimization on the basis of a target function comprising only the following four terms: experimental dipolar coupling restraints (18 for each subunit), distance restraints to link the A (A′) and B (B′) halves of each subunit and to prevent steric clash, a radius of gyration (R_{gyr}) restraint to achieve appropriate compaction (see below), and a quartic van der Waals repulsion term. The X-ray coordinates for the AB′ half of the dimer are fixed; the A′B half of the dimer (X-ray coordinates) is allowed to rotate and translate (6 degrees of freedom), while the axes of the alignment tensor are free to rotate (3 degrees of freedom). The covalent

---

(19) The sign of the $^1D_{NH}$ dipolar couplings in the present paper takes into account the fact that the $^1J_{NH}$ couplings are negative. In ref 2, the $^1D_{NH}$ couplings were simply taken as the difference between the absolute values of $^1J_{NH}$ in the liquid crystal and isotropic media, so that the sign of D_a^{NH} reported for the monomer in ref 2 is opposite to that given in the present paper.
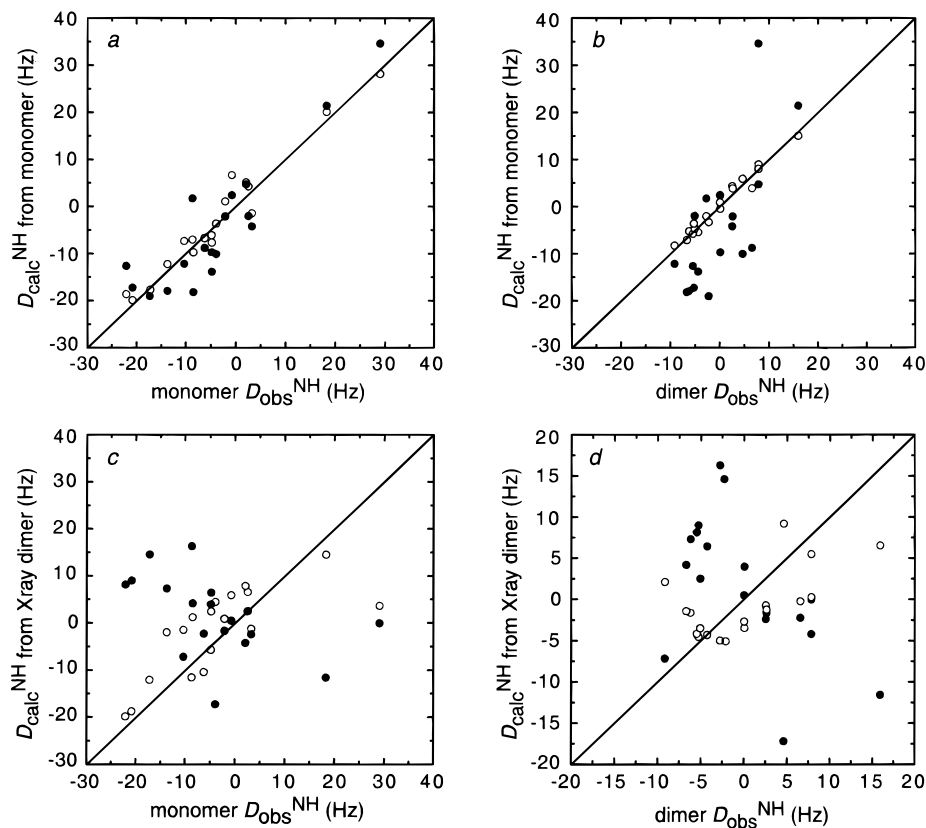
Figure 3. Comparison of the experimentally measured dipolar couplings (D_{obs}^{NH}) for the monomer (a and c) and the dimer (b and d) with the values (D_{calc}^{NH}) calculated by best-fitting using SVD (O) or predicted from the molecular shape (●) on the basis of the X-ray coordinates of the monomer (a and b) and dimer (c and d). Note the coordinates of the monomer are given by the A′B half of the dimer. The dipolar couplings plotted for the monomer are restricted to those residues for which dipolar couplings could be measured on the dimer.

restraints consist of 4×2 distance restraints: specifically, the Cα−Cα distance between residues 49 and 52 and residues 50 and 53 is restrained to a range of 8.5−11.0 Å, and that between residues 48 and 52 and residues 49 and 53, to a range of 9.0−13.3 Å. In addition, there are four distance restraints to prevent steric clash between the AB′ and A′B halves of the dimer: specifically, the Cα−Cα distances between residues 50 and 50′ and residues 52 and 52′ are restrained to be greater than 6 Å apart, and between residues 38 and 52 and residues 38′ and 52′ greater than 4 Å apart. The R_{gyr} restraint provides long-range translational information.[14] Because we do not know a priori what the radius of gyration should be (since this will be critically dependent on the relative orientation of the two halves of the dimer), we carried out a grid search by performing a series of calculations with the target value for the radius of gyration, Rgyr(target), incremented from 16 to 19.5 Å.[20] Since the dipolar couplings measured on the dimer must agree with both the monomer (i.e., AB′ half of the dimer in isolation) as well as the dimer (i.e., AB′ and A′B halves combined), the values of D_a^{NH} (7.6 Hz) and η (0.2) employed in the calculations were those obtained by an SVD best-fit to the X-ray coordinates of the AB′ half of the dimer (Figure 3b). In the starting coordinates, the separation between the AB′ and A′B halves of the dimer is ∼45 Å and the linker residues, Pro51 and Pro51′, are deleted (to permit free rotation and translation of A′B relative to AB′). Three different starting orientations of the A′B half relative to AB′ half were employed: antiparallel, parallel, and the X-ray orientation (Figure 4). The calculations starting from the antiparallel and X-ray orientations converged to identical structures, while those starting from the parallel orientation converged to an alternate orientation related by an approximately 180° rotation from the former.

Dipolar couplings measured from a single alignment tensor will be consistent with four possible orientations of the A′B half of the dimer relative to that of the AB′ half. However, the requirement that the separation between residues 50 and 52 and residues 50′ and 52′ be consistent with a covalent link between A and B and between A′ and B′ bridged by the deleted Pro51 and Pro51′, respectively, reduces the number of solutions consistent with the dipolar couplings to two that differ by approximately 180° (cf. Figures 5, 8, and 9). We will refer to these as the antiparallel and parallel solutions. Stereoviews showing the antiparallel and parallel solutions calculated for different values of R_{gyr}(target) are shown in Figure 5a and b, respectively. Figure 6 plots the agreement between the calculated dipolar couplings (using both SVD and back-calculation on the basis of molecular shape) with the observed dipolar couplings for the dimer (Figure 6a and b), the magnitude of the calculated alignment tensors (obtained both by SVD and back-calculation from molecular shape) (Figure 6c and d), and the actual value of R_{gyr} (Figure 6e) as a function of R_{gyr}(target). Figure 7 provides a plot of predicted dipolar couplings back-calculated from molecular shape versus observed dipolar couplings for the different values of R_{gyr}(target).

In the case of the antiparallel solution (Figures 5a and 9a), the agreement between the observed dipolar couplings and those calculated using SVD is good and displays little sensitivity to R_{gyr}(target) with the rmsd (Figure 6a) and linear correlation coefficient (Figure 6b) ranging from 1.2 Hz and 0.98, respectively, for R_{gyr}(target) = 19.5 Å to 1.5 Hz and 0.9, respectively, for R_{gyr}(target) = 16.0 Å. (Note that the minimum value of R_{gyr} actually attained is 17.6 Å since there is a physical limit to the degree of compaction, owing to the presence of the van der Waals repulsion term in the target function, Figure 6e.) On the
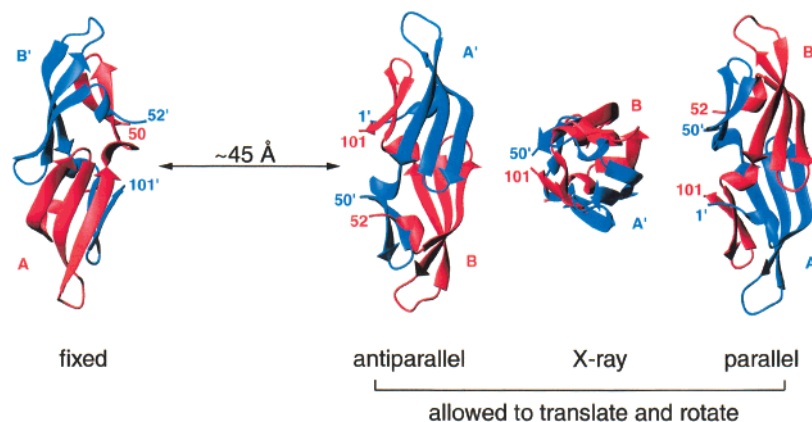
Figure 4. Starting coordinates for the rigid body minimization calculations. The AB′ half of the dimer is separated by ∼45 Å from the A′B half, and the linker residues, Pro51 and Pro51′, are deleted. Three different orientations of A′B relative to those of AB′ were used, namely antiparallel, X-ray and parallel orientations. In the rigid body minimization calculations AB′ is fixed, while A′B is allowed to translate and rotate.
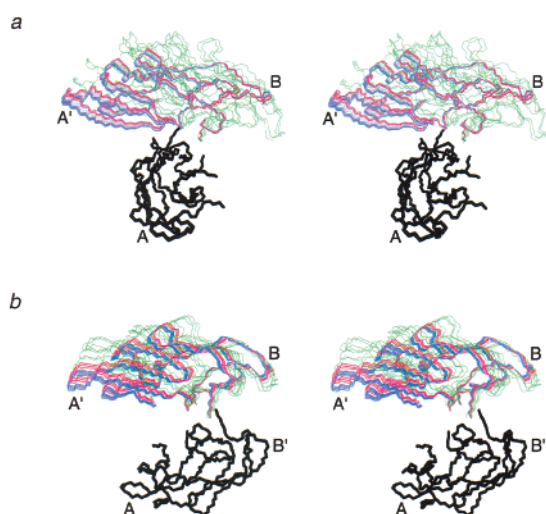
Figure 5. Stereoviews showing superpositions of the structures obtained by rigid body minimization for different values of R_{gyr}(target). The antiparallel and parallel solutions are shown in (a) and (b), respectively. The antiparallel solutions are obtained starting from the coordinates with A′B either antiparallel or in the X-ray orientation relative to AB′, while the parallel solutions are obtained starting from the coordinates with A′B parallel to AB′ (see Figure 4). The AB′ half of the domain-swapped dimer (which is always held fixed) is shown in black. The color coding employed for the A′B half of the dimer is as follows: structures in blue are calculated with R_{gyr}(target) = 16.0, 16.25, 16.5, and 16.75 Å; in red with R_{gyr}(target) = 17.0 17.25, and 17.5 Å; and in green with R_{gyr}(target) = 18.0, 18.5, 19.0, and 19.5 Å. Also shown in (a) is a collection of 20 structures in gray calculated with R_{gyr}(target) = 17.25 Å using 20 different sets of dipolar couplings to which random noise ranging from 1.5 to 2 Hz had been added to the measured dipolar couplings for the dimer.

other hand, the agreement between the observed dipolar couplings and those predicted from the molecular shape displays a strong dependence on the value of R_{gyr}(target) (Figure 6a and b, Figure 7a and c). For R_{gyr}(target) ≤ 17.5 Å, the rmsd and correlation coefficient have values ≤2.1 Hz and ≥0.96, respectively, and have their minimum and maximum values, respectively, for R_{gyr}(target) = 17.25 Å. The angle between the AB′ and A′B halves of the dimer lies in the range 105−110° for these structures. As R_{gyr}(target) increases beyond 18 Å, the agreement worsens considerably such that for R_{gyr}(target) = 19.5 Hz, the rmsd and correlation coefficient have values of 9.5 Hz and 0.48, respectively. While the value of D_a^{NH} calculated by SVD varies little as a function of R_{gyr}(target), the predicted value

back-calculated from the molecular shape shows a clear variation, lying in the range 6.0−6.9 Hz for R_{gyr}(target) ≤ 18.5 and increasing up to 12.7 Hz for R_{gyr}(target) = 19.5 Å. This increase in the predicted value of D_a^{NH} back-calculated from the molecular shape signifies that the molecule becomes more prolate as R_{gyr}(target) increases beyond 19 Å (cf. Figure 5a).

In the case of the parallel solution (Figures 5b and 9b), the agreement between the dipolar couplings calculated by SVD and the observed dipolar couplings improves as R_{gyr}(target) increases, from an rmsd and correlation coefficient of 2.6 Hz and 0.92, respectively, for R_{gyr}(target) = 16 Å to 1.3 Hz and 0.98, respectively, for R_{gyr}(target) = 19.5 Å (Figure 6a and b). The value of D_a^{NH} calculated by SVD varies over a very small range (7.5 to 7.6 Hz) as a function of R_{gyr}(target) (Figure 6c). The agreement, however, with the dipolar couplings predicted from the molecular shape, is very poor for all values of Rgyr(target) (Figure 7b and d) with the rmsd ranging from 9.4 to 14.7 Hz (Figure 6a) and the correlation coefficient ranging from 0.73 to 0.4 (Figure 6b) as R_{gyr}(target) is increased from 16 to 19.5 Å. Moreover, the predicted value of D_a^{NH} back-calculated from the molecular shape is negative, ranging from −14.7 to −17.2 Hz (Figure 6c). Thus, the parallel solution yields a dimer which is oblate in shape (Figure 9b).

From the above data, we can conclude that the antiparallel solutions obtained with R_{gyr}(target) ranging from 16 to 17.5 Å are representative of the structure of the dimer at neutral pH. Although, the structures calculated for R_{gyr}(target) ≥ 18 Å display slightly smaller rmsd's between observed and SVD calculated dipolar couplings, the improvement is insignificant. Thus, the rmsd for R_{gyr}(target) = 19.5 Å is 1.2 Hz, while that for R_{gyr}(target) = 17.25 Å (which corresponds to the minimum obtained by back-calculation from molecular shape) is 1.4 Hz (Figure 6a), and the correlation coefficient (0.98) is the same in both cases (Figure 6b). Thus, there is a range of orientations that is consistent with the measured dipolar couplings which can be reduced to a narrow window by the application of back-calculation on the basis of molecular shape (Figure 5a).

The measured dipolar couplings contain random error (estimated at around ±1 Hz). Since the number of measured dipolar couplings for the dimer is relatively small (18 × 2), we also investigated the effect of random noise. A set of 20 structures were calculated with random noise ranging from 1.5 to 2 Hz added to the dipolar couplings using R_{gyr}(target) set to 17.25 Å. As is evident from Figure 5a, the introduction of noise had no significant impact since all the resulting structures fall within
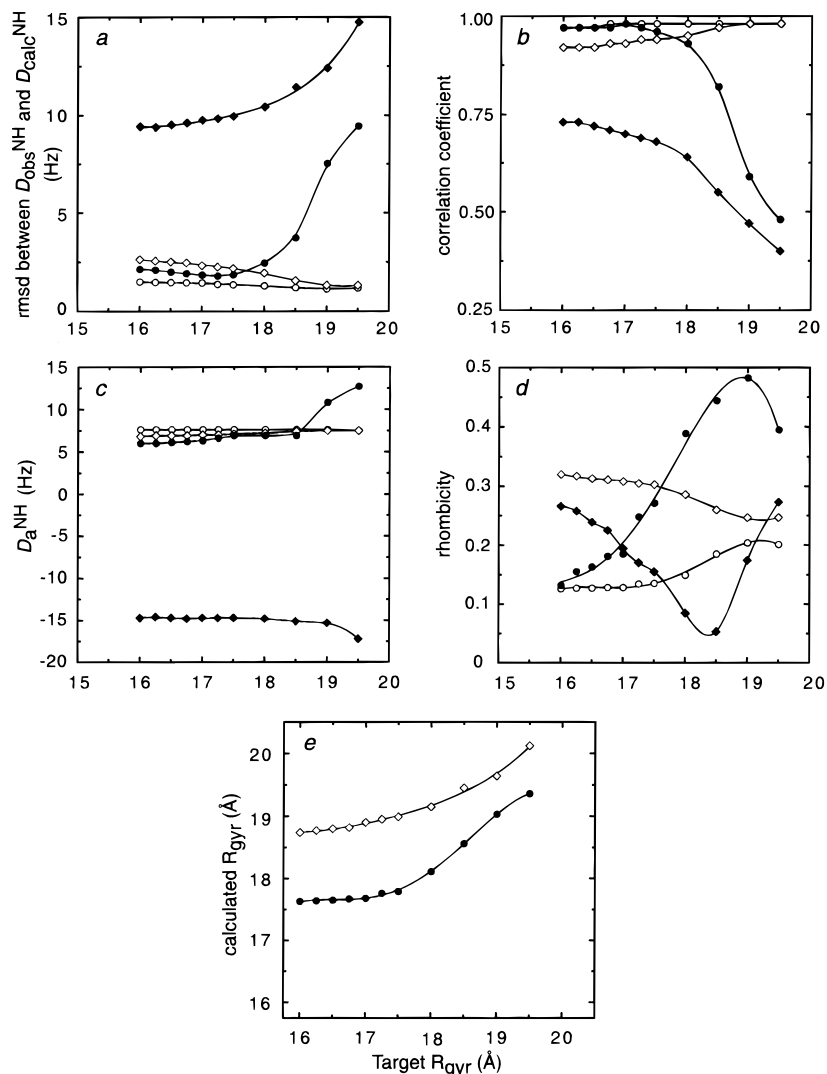
Figure 6. Agreement between observed (D_{obs}^{NH}) and calculated (D_{calc}^{NH}) dipolar couplings (a and b), magnitude (D_a^{NH} and rhombicity) of the calculated alignment tensor (c and d), and calculated value of R_{gyr} as a function of Rgyr(target). The antiparallel solutions are displayed as circles and the parallel ones as diamonds; in panels (a) to (d) the solid symbols refer to parameters back-calculated from molecular shape, and open symbols refer to parameters calculated by SVD. The agreement between observed and calculated dipolar couplings is measured by the rmsd between the observed and calculated values (a) and the linear correlation coefficient (b).

the conformational space sampled by the structures calculated with R_{gyr}(target) ranging from 16 to 17.5 Å.

Another source of error lies in the values used for D_a^{NH} and η in the rigid body minimization, since these parameters are fixed in the calculation and only the orientation of the tensor is allowed to change. As indicated above, we used the values obtained by an SVD fit to the monomer coordinates. To investigate the effect of the value of D_a^{NH} and η used in the calculations, we carried out a grid search (with R_{gyr}(target) set to 17.25 Å) in which a series of structures were calculated for values of D_a^{NH} and η ranging from 6.0 to 12.0 Hz (in increments of 0.5 Hz) and from 0.0 to 0.6 (in increments of 0.1), respectively. The rmsd between the observed dipolar couplings and those calculated by rigid body minimization (i.e., D_a^{NH} and η fixed, with the orientation of the alignment tensor allowed to change) ranges from 1.5 Hz for $D_a^{NH} = 7.5$ Hz and $\eta = 0.1$, to 5.0 Hz for $D_a^{NH} = 12$ Hz and $\eta = 0.6$. The values of D_a^{NH} and η calculated by SVD from the resulting coordinates, however, display little variation ranging from 7.6 to 7.7 Hz and 0.12 to 0.18, respectively, with an rmsd and correlation coefficient ranging from 1.4 to 1.6 Hz and from 0.97 to 0.98, respectively. Likewise the predicted values of D_a^{NH} and η back-calculated

from the molecular shape range from 4.4 to 6.8 Hz and from 0.1 to 0.27, respectively, with an rmsd and correlation coefficient ranging from 1.8 to 3.8 Hz and from 0.98 to 0.87. Even for D_a^{NH} and η set to either 6.0 Hz and 0, or 12.0 Hz and 0.6 in the rigid body minimization calculations, the rotation required to fit the A′B half of the dimer onto that obtained for the values of D_a^{NH} and η used in all of the other calculations (7.6 Hz and 0.2) is only 6 and 15°, respectively. Thus, the structure is relatively insensitive to the choice of D_a^{NH} and η used in the rigid body minimization calculations. The reason for this lies in the strict requirement arising from C_2 symmetry that one of the axes of the alignment tensor lie parallel and the other two orthogonal to the symmetry 2-fold axis.

A superposition of the antiparallel and parallel dimer structures obtained by rigid body minimization onto the X-ray dimer (with best-fitting of the AB′ half of the molecule) is shown in Figure 8, and a comparison of the three structures is shown by a set of two mutually orthogonal views in Figure 9. The relative orientations of the two halves of the dimer in the three structure differ in terms of both orientation and translation as a consequence of the distance restraints used to ensure that the separation of residues 50 and 52 and residues 50′ and 52′ are
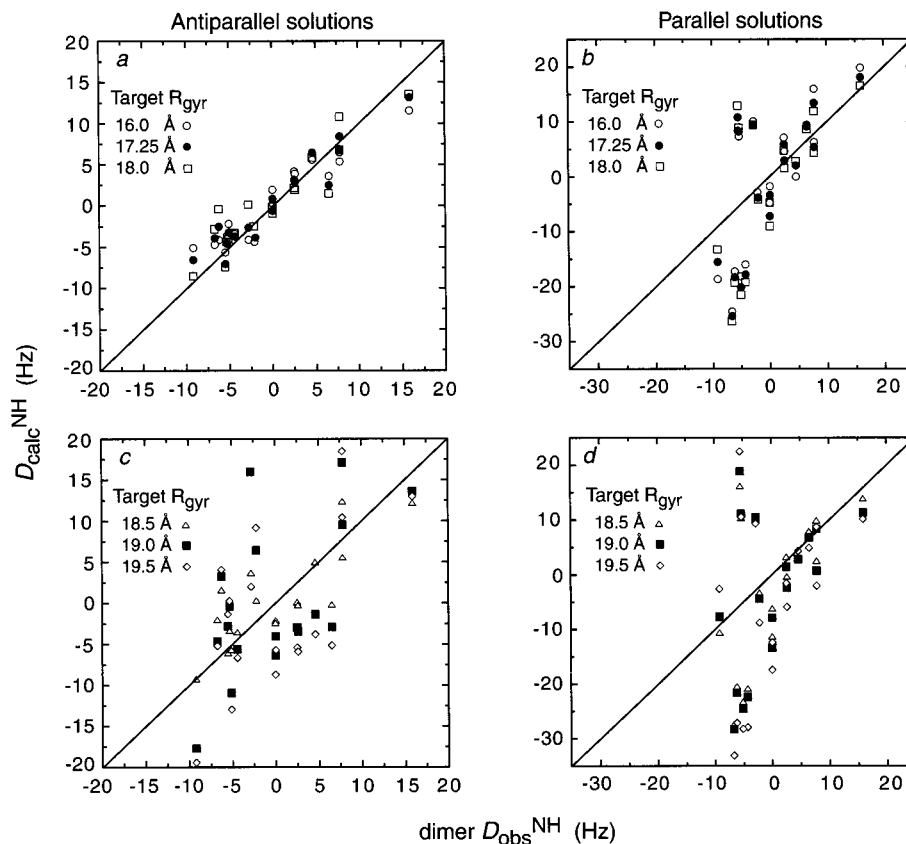
Figure 7. Correlation between the observed dipolar couplings (D_{obs}^{NH}) and the predicted dipolar couplings back-calculated from the molecular shape for different values of R_{gyr}(target). The results for the antiparallel solutions are given in the left-hand panels (a and c) and those for the parallel solutions in the right-hand panels (b and d). Only the antiparallel solutions with R_{gyr}(target) set in the range 16–17.5 Å are consistent with the predicted dipolar couplings back-calculated from the molecular shape of the dimer.
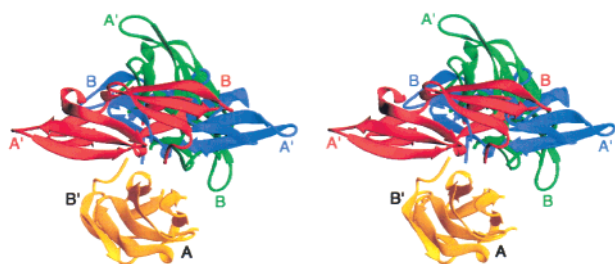
Figure 8. Stereoview showing a best-fit superposition to the AB′ half of the dimer for the antiparallel and parallel solutions and X-ray structure. The AB′ half (which is fixed and identical for all three cases) is shown in gold. The A′B half for the antiparallel solution [R_{gyr}(target) = 17.25 Å] is shown in red, the parallel solution [R_{gyr}(target) = 17.25 Å] in blue, and the X-ray structure in green. Only the antiparallel solution is consistent with the predicted dipolar couplings back-calculated from the molecular shape of the dimer.

sufficiently close to be compatible with a covalent link of A to B and A′ to B′ bridged by Pro51 and Pro51′, respectively. The angle between the long axes of the two halves of the dimer (AB′ and A′B) is ∼110° for the antiparallel solution, ∼−40° for the parallel solution and ∼80° for the X-ray dimer. In principle the antiparallel and parallel solutions should differ by a 180° rotation. However, for the optimal solution at R_{gyr}(target) = 17.25 Å, the difference in orientation is only ∼150° owing to steric clash. This angle is increased to ∼170° if the antiparallel structure calculated with R_{gyr}(target) = 17.25 Å is compared to the parallel one calculated with R_{gyr}(target) = 19.5 Å. From Figure 9, the difference in shape for the three domain-swapped dimers is clearly apparent: the antiparallel solution is prolate in shape, consistent with the measured dipolar couplings,
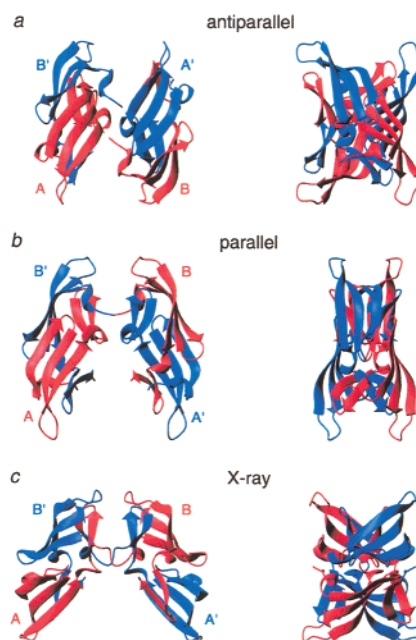
Figure 9. Two orthogonal views illustrating ribbon diagrams of (a) the antiparallel solution, (b) the parallel solution, and (c) the X-ray structure (c). The antiparallel and parallel solutions shown are those obtained with R_{gyr}(target) = 17.25 Å. Only the antiparallel solution is consistent with the predicted dipolar couplings back-calculated from the molecular shape of the dimer.

whereas the parallel solution and the X-ray structure are oblate which is inconsistent with the measured dipolar couplings.

Concluding Remarks

We have shown that the orientation of the two halves (AB′ and A′B) of the domain-swapped dimer and, consequently, the overall shape of the dimer at neutral pH in solution (Figure 9a) are different from those observed in the X-ray structure (Figure 9c) obtained from crystals grown at low pH in 26% 2-propanol. Using back-calculation of dipolar couplings based on molecular shape, we were able to distinguish between two possible orientations (antiparallel and parallel) that differ by ~180° and narrow the range of orientations within the antiparallel set (calculated with R_{gyr}(target) values ranging from 16 to 19.5 Å) to a very narrow window (Figures 5−7).

What factors stabilize the dimer orientation in solution, particularly since the contacts between the A′B and AB′ halves of the dimer are rather limited? In the crystal structure there is a hydrogen bond between the neutral carboxylate of Glu41 of one subunit and of Glu41′ of the other (Figure 1b), supplemented by a water-bridged hydrogen bond between the hydroxyl of Tyr100 and the backbone carbonyl of Gln50′, and a van der Waals contact between the aliphatic portion of the side chains of Gln50 and Gln50′ (which are separated by only ~2 Å). There are no further contacts between the two halves of the dimer in the crystal structure. However, one-half of a neighboring dimer inserts itself between the two halves of the dimer in the crystal lattice (Figure 1b) and must therefore be considered a major determinant of the relative orientations of the two halves of the dimer observed in the crystal. At neutral pH, where the carboxylate is negatively charged, the side chains of Glu41 and Glu41′ will repel each other. This, together with the absence of crystal packing, leads to a reorientation of the two halves of the domain-swapped dimer in solution as can be seen in Figure 8 and by comparing Figure 9a and c. In the antiparallel orientation (in which the angle between the two halves of the dimer is ~110°, Figure 9a), there are several hydrogen bonding interactions between the two halves of the dimer: specifically, there are potential hydrogen bonds between the carboxylate of Asp35 and the backbone amide of Asp35′, the side chain of Asn37 and the hydroxyl group of Ser38′, the side chains of Gln50 and Gln50′, and the aromatic ring of Tyr100 and the hydroxyl of Ser52′, as well as a few hydrophobic interactions such as those between the aliphatic portions of Ser38 and Ser38′, and between Ser52 and Val39′.

In conclusion, we have shown that the combined use of a small number of orientational and translational restraints in conjunction with rigid body minimization and appropriate filtering achieved by back-calculation of dipolar couplings on the basis of molecular shape can be used to determine the relative orientations of two halves of a symmetric dimer. The approach presented here should find a wide range of applicability to numerous other structural problems involving multimeric proteins and protein−protein complexes.

Experimental Section

Expression and purification of uniformly (>95%) ^{15}N-labeled CVN was carried out as described previously.[2] Samples for NMR contained ~1 mM protein at pH 6.1. All NMR experiments were carried out on a Bruker DMX600 spectrometer. One bond [1]H−[15]N dipolar couplings, [1]D_{NH}, were measured at 38 °C by taking the difference in the [1]J_{NH} splittings measured on oriented (in 4.5% 3:1 DMPC:DHPC) and isotropic (in water) CVN. [1]J_{NH} couplings were obtained by recording a 2D IPAP {[15]N−^{1}H} HSQC experiment[21] to generate two spectra containing either the upfield or downfield component of the ^{15}N doublet component.

Structure calculations using rigid body minimization were carried out with the program XPLOR[22] using exactly the same protocol described in ref 13, with the exception that additional cycles of rigid body minimization (300 steps) were added at the end of the protocol with the additional term for the radius of gyration (R_{gyr})[14] included in the target function. The value of R_{gyr}(target) was decreased incrementally, starting at 19.5 Å and ending up at 16 Å. The X-ray coordinates were used for the AB′ (residues 1−50 of subunit 1 and residues 52′−101′ of subunit 2) and A′B (residues 1′−50′ of subunit 2 and residues 52−101 of subunit 1) halves of the domain-swapped dimer (PDB accession code 3ezm).[3]

Singular value decomposition (SVD), as implemented in the program SSIA,[15] was used to best-fit the alignment tensor to the observed [1]D_{NH} couplings on the basis of the coordinates.[18] Prediction of the net alignment tensor on the basis of molecular shape was carried out using the program SSIA as described in ref 15. Since the alignment of the protein in a liquid crystalline medium, in the absence of any attractive or long-range repulsive interactions between the protein and the liquid crystal particles, is dominated by an obstruction effect, this involves averaging all individual alignment matrices calculated for each non-obstructed position and orientation of the protein.[15]

(20) The expected R_{gyr} for a globular protein of 202 residues (i.e. the total number of residues for the dimer) would be expected to be $2.2 \times 202^{0.38} = 16.5$ Å.[14] However, the contact area between the two halves of the dimer is very small, and hence the dimer itself is not globular. Thus, the actual R_{gyr} would be expected to be larger than that predicted from the number of residues. For the X-ray structure the value of R_{gyr} is 19.6 Å. We therefore carried out a series of calculations with R_{gyr}(target) set to 16.0, 16.25, 16.5, 16.75, 17.0, 17.25, 17.5, 18.0, 18.5, 19.0, and 19.5 Å as well as one calculation with no R_{gyr} restraint. The minimum value of R_{gyr} actually attained is 17.6 Å for the antiparallel solution and 18.7 Å for the parallel solution (Figure 6e). The Cα atomic rms difference between the structures calculated with no R_{gyr} restraint and R_{gyr}(target) = 19.5 Å, is 0.6 Å for the antiparallel solution and 0.8 Å for the parallel solution.
(21) Ottiger, M.; Delaglio, F.; Bax, A. *J. Magn. Reson.* **1998**, *131*, 173−178.
(22) Brünger, A. T. *XPLOR: A System for X-ray Crystallography and NMR*; Yale University Press: New Haven, CT, 1993.